

Do stellar magnetic cycles influence the measurement of precise radial velocities?★,★★

N. C. Santos^{1,2}, J. Gomes da Silva^{1,2}, C. Lovis³, and C. Melo⁴

¹ Centro de Astrofísica, Universidade do Porto, Rua das Estrelas, 4150-762 Porto, Portugal
e-mail: nuno@astro.up.pt

² Departamento de Matemática Aplicada, Faculdade de Ciências da Universidade do Porto, Portugal

³ Observatoire de Genève, 51 ch. des Maillettes, 1290 Sauverny, Switzerland

⁴ European Southern Observatory, Casilla 19001, Santiago 19, Chile

Received 9 October 2009 / Accepted 14 December 2009

ABSTRACT

The ever increasing level of precision achieved by present and future radial-velocity instruments is opening the way to discovering very low-mass, long-period planets (e.g. solar-system analogs). These systems will be detectable as low-amplitude signals in radial-velocity (RV). However, an important obstacle to their detection may be the existence of stellar magnetic cycles on similar timescales. Here we present the results of a long-term program to simultaneously measure radial-velocities and stellar-activity indicators (CaII, H α , HeI) for a sample of stars with known activity cycles. Our results suggest that all these stellar activity indexes can be used to trace the stellar magnetic cycle in solar-type stars. Likewise, we find clear indications that different parameters of the HARPS cross-correlation function (BIS, FWHM, and contrast) are also sensitive to activity level variations. Finally, we show that, although in a few cases slight correlations or anti-correlations between radial-velocity and the activity level of the star exist, their origin is still not clear. We can, however, conclude that for our targets (early-K dwarfs) we do not find evidence of any radial-velocity variations induced by variations of the stellar magnetic cycle with amplitudes significantly above ~ 1 m/s.

Key words. planetary systems – stars: fundamental parameters – techniques: spectroscopic – techniques: radial velocities – stars: activity – starspots

1. Introduction

Following the discovery of the first extrasolar planet orbiting a solar type star (Mayor & Queloz 1995), a multitude of other planetary systems have been announced (for a review see Udry & Santos 2007). At first, only very short-period companions were found, something that was quite unexpected by the theories of giant planet formation. However, the impressive increase in precision of the current radial-velocity (RV) “machines” (the majority of the established exoplanets have been discovered by radial-velocity surveys) and the long baseline of the measurements have already brought to light both long-period planets, much more similar to the Solar System giants (e.g. Wright et al. 2008), and very low-mass rocky planets (e.g. Mayor et al. 2009).

Although extremely efficient, the RV technique is an indirect method, and it does not allow direct detection of a planet, but only measures the (gravitational) stellar wobble induced by the planetary companion orbiting its sun. As a consequence, one of the problems is that one has to assure that the radial-velocity variations observed are not being caused by some other mechanism unrelated to the presence of a low-mass companion.

Phenomena such as stellar pulsation (e.g. Bouchy et al. 2004), inhomogeneous convection, or spots (Saar & Donahue 1997; Santos et al. 2000; Paulson et al. 2002) can prevent us from finding planets (if the perturbation is stronger than the orbital radial-velocity variation); but perhaps more important, they might give us false candidates if they produce a periodic signal (Queloz et al. 2001; Bonfils et al. 2007; Huélamo et al. 2008). In other words, the radial-velocity technique is sensitive not only to the motion of a star around the center of mass of a star/planet system, but also to possible variations in the structure of the stellar surface.

This matter is getting more important every day. One clear output of the increase in precision of the current radial-velocity surveys is the ability to find low-mass and long-period planets, that are able to induce long-period but low-amplitude radial-velocity signals. These expected Jupiter-analogs might be easily found e.g. with instruments like HARPS (Pepe et al. 2002) and with future instrumentation like the projected ESO instruments ESPRESSO¹ and CODEX (Pasquini et al. 2008). But if in these cases stellar rotational effects are not potentially dangerous (rotational periods are much shorter than the long-period Jupiter orbit), another almost quantitatively unknown effect might threaten these detections: stellar activity cycles.

It is now well known that many solar type stars have important magnetic activity cycles (Baliunas et al. 1995), similar to the solar 22-year period (11+11 period spot cycle). These cycles have timescales comparable to the orbital periods of real Jupiter

* Based on observations collected at the La Silla Parana Observatory, ESO (Chile) with the HARPS spectrograph at the 3.6-m telescope (ESO runs ID 072.C-0096 073.D-0038 074.D-0131 075.D-0194 076.D-0130 078.D-0071 079.D-0075 080.D-0086 081.D-0065)

** Tables 5 to 8, with the data used for Figs. 2, 3, and 8, are available in electronic form at the CDS via anonymous ftp to cdsarc.u-strasbg.fr (130.79.128.5) or via <http://cdsweb.u-strasbg.fr/cgi-bin/qcat?J/A+A/511/A54>

¹ <http://espresso.astro.up.pt>

Table 1. Basic data for our stars and observation log.

Star	V	$B - V$	Sp. type	P_{rot} [days]	First observation	Last observation	# nights	$\langle S/N \rangle$
HD 4628	5.74	0.890	K2V	39	2003-10-26	2008-09-05	36	34
HD 16160	5.79	0.918	K3V	48	2003-10-26	2008-09-05	43	28
HD 26965A	4.43	0.820	K1V	43	2003-10-26	2008-09-05	38	43
HD 32147	6.22	1.049	K3V	47	2003-10-26	2008-09-05	35	24
HD 152391	6.65	0.749	G8V	11	2003-06-18	2008-09-11	38	36
HD 160346	6.53	0.959	K3V	37	2004-02-10	2008-09-11	31	29
HD 216385	5.16	0.487	F7IV	7	2003-10-26	2008-09-11	29	56
HD 219834A	5.20	0.787	G6/G8IV	42	2003-10-26	2008-07-09	25	48

like planets. In this sense, RV measurements of the Sun during a 5-year period have revealed that “our” star might be stable up to a precision of a few m/s (McMillan et al. 1993). However, no tests have been done regarding other solar-type stars. Some effect of the activity level on the radial-velocity might indeed be expected. It is known that magnetic fields are able to change the convection patterns (e.g. inhibiting convection), thus changing line bisectors and line shifts (Dravins 1982). But with the exception of a very few cases (Kürster et al. 2003, for Barnard’s star, an M dwarf), it is not really known or accurately explored, to which level the line asymmetries induced by changes in the convection patterns throughout the stellar magnetic cycles can influence the measurement of precise radial velocities.

In this paper we present a study of the relation between long-term chromospheric activity variations, RV, and different line profile indicators. In Sect. 2 we present our sample and observations, and in Sect. 3 we derive precise atmospheric parameters and masses for our stars. In Sect. 4 we then present the methodology used to derive the stellar activity level of our stars from each obtained spectrum. The analysis of the data and the presentation of the results is done in Sect. 5. We conclude in Sect. 6.

2. Sample and observations

The choice of our targets was based on the sample of stars followed within the Mount Wilson project to study the magnetic cycle variations in nearby FGK stars (Vaughan et al. 1978; Baliunas et al. 1995). In particular, we based our choice on the sample presented in Baliunas et al. (1995). From the stars and results presented by these authors, we first took those showing clear activity cycles. Then, only objects at a declination south of +10 degrees were considered, in order to be able to follow them from the La Silla observatory (the site of HARPS) for several months each year. One star that presented a particularly stable activity level was also chosen as the standard (HD 216385).

In Table 1 we list the stars in our sample with their V magnitudes, $B - V$ colors, and spectral types. The values were taken from the Hipparcos catalog (ESA 1997). Rotational periods were taken from Baliunas et al. (1996). As we can see from the table, most stars are late-G or early-K dwarfs, with the exception of HD 216385 (late F) and HD 219834A (likely a subgiant) – see also Table 2.

To allow for a continuous follow-up of each target, observations were done in service mode starting from September 2003 (ESO period 72), just when HARPS became available. All stars were followed until September 2008 (ESO period 81). No more follow-up was then possible due to the end of service-mode observations at La Silla. For HD 152391, one extra measurement done during the commissioning of HARPS (June 2003) was added.

In general, each star was observed in 5 different epochs during each observing season (6 months). An effort was made to spread the observations in time as much as possible. This was important to allow us to average any strong variations due to rotational modulation effects out. We are interested in studying the effects of long term magnetic cycle variations.

Every measurement was done with the high-precision simultaneous calibration mode. Though the use of the Thorium-Argon simultaneous calibration may complicate the subtraction of scattered light over the whole image (specially in the blue part of the spectrum where the spectral orders are separated by only a few pixels), this mode was judged important since we need m/s precision in our measurements.

Stellar oscillations can induce significant radial-velocity signals on timescales of a few minutes. In order to average the stellar oscillation modes out (e.g. Santos et al. 2004a), each measurement was done with a total exposure time of 15 min. For the brightest stars in our sample, this implies several shorter exposures to avoid CCD saturation.

Individual RVs were derived with the HARPS pipeline. The velocities were derived using the cross-correlation function (CCF) method. The bisector inverse slope (BIS) was derived using the methodology described in Queloz et al. (2000). Other parameters of the CCF, such as the contrast and FWHM, were also computed.

3. Spectroscopic stellar parameters and masses

With the combined HARPS spectra, we derived stellar parameters and metallicities for the sample stars using the methodology and line-lists described in Santos et al. (2004b) and Sousa et al. (2008), respectively. Equivalent widths of individual Fe I and Fe II lines were measured with the automatic code ARES². A grid of Kurucz (1993) model atmospheres was adopted together with the 2002 version of the radiative transfer code MOOG (Snedden 1973). We point the readers to Santos et al. (2004b) for more details on the technique. In Table 2 we list the final derived values, together with the number of Fe I and Fe II lines used and their dispersion. For comparison, the astrometric surface gravity was also derived using Eq. (1) in Santos et al. (2004b). Both estimates of the surface gravity agree well within the errors.

Stellar masses were also derived by interpolating the theoretical isochrones of Schaller et al. (1992), Schaerer et al. (1993a), and Schaerer et al. (1993b), using M_V computed using Hipparcos parallaxes (ESA 1997), a bolometric correction from Flower (1996), and the T_{eff} obtained from the spectroscopy. The results are also listed in Table 2. We estimate that the uncertainties are around 10% because of errors in the input parameters and

² <http://www.astro.up.pt/~sousasag/ares>

Table 2. Stellar parameters derived for the stars in our sample.

Star	T_{eff} [K]	$\log g_{\text{spec}}$ [cm s^{-2}]	ξ_t [km s^{-1}]	[Fe/H]	$N(\text{Fe I}/\text{Fe II})$	$\sigma(\text{Fe I}/\text{Fe II})$	$\log g_{\text{hipp}}$ [cm s^{-2}]	Mass [M_{\odot}]
HD 4628	5044 ± 52	4.54 ± 0.36	0.53 ± 0.18	-0.32 ± 0.11	257/31	0.11/0.16	4.61	0.72
HD 16160	4921 ± 103	4.54 ± 0.54	0.46 ± 0.43	-0.16 ± 0.19	258/32	0.18/0.24	4.58	0.69
HD 26965A	5136 ± 50	4.46 ± 0.30	0.44 ± 0.15	-0.32 ± 0.09	258/32	0.09/0.13	4.42	0.65
HD 32147	4902 ± 136	4.33 ± 0.73	0.60 ± 0.54	0.21 ± 0.21	259/34	0.19/0.34	4.62	0.79
HD 152391	5474 ± 25	4.46 ± 0.19	1.01 ± 0.04	-0.04 ± 0.06	256/33	0.06/0.08	4.56	0.92
HD 160346	4998 ± 68	4.44 ± 0.38	0.81 ± 0.17	-0.08 ± 0.14	258/32	0.14/0.18	4.63	0.78
HD 216385	6371 ± 30	4.24 ± 0.34	1.63 ± 0.04	-0.13 ± 0.06	230/36	0.06/0.12	4.06	1.36
HD 219834A	5530 ± 41	3.95 ± 0.17	1.06 ± 0.04	0.13 ± 0.11	257/34	0.11/0.07	3.96	1.25

Table 3. Average chromospheric activity indexes derived using the Ca II H and K lines, with the values presented in Baliunas et al. (1995) presented for comparison.

Star	$\langle S_{\text{MW}} \rangle_{\text{(ours)}}$	$\langle S_{\text{MW}} \rangle_{\text{(Baliunas)}}$	$\langle \log R'_{\text{HK}} \rangle_{\text{(ours)}}$
HD 4628	0.22	0.230	-4.89
HD 16160	0.23	0.226	-4.88
HD 26965A	0.19	0.206	-4.92
HD 32147	0.28	0.286	-4.95
HD 152391	0.39	0.393	-4.44
HD 160346	0.31	0.300	-4.78
HD 216385	0.15	0.142	-5.00
HD 219834A	0.16	0.155	-5.03

also because of different systematic effects (Fernandes & Santos 2004).

A look at Table 2 shows that all but one of the targets are main sequence dwarfs. The exception is HD 219834 A, most likely a subgiant.

4. Activity indexes

From each individual spectrum, stellar activity indexes were derived using three different indicators: the Ca II H and K lines, the H_{α} line, and the He I D3 line at 5875.6 Å. All activity indexes were derived following the general procedures described in Santos et al. (2000, for the Ca II lines) and Boisse et al. (2009, for H_{α} and He I). All the activity level derivations used the pipeline reduced and wavelength calibrated 2-dimensional spectra. Individual errors were derived with the number of counts in each wavelength region.

The Ca II H and K “ S_{HARPS} ” index was computed by dividing the sum of the flux in two 1 Å wide intervals in the center of each line (at 3933.66 and 3968.47 Å, respectively), by the flux in two 20 Å wide reference windows centered on 3900.0 and 4000.0 Å. A weighted sum took the photon noise errors derived as \sqrt{N} into account (with N the number of counts). Once all the spectra were analyzed, an average S_{HARPS} value was derived for each star. Its value was then used to calibrate the S_{HARPS} values to the Mount-Wilson scale. For this calibration we used the S_{MW} values listed in Baliunas et al. (1995)³ – see Table 3. Finally, using the relation in Noyes et al. (1984), we could derive the values of the Ca II flux corrected for the photospheric flux, $\log R'_{\text{HK}}$.

In Table 3 we list the average values for each of our targets (both for S_{MW} and $\log R'_{\text{HK}}$), together with the values for the S_{MW} listed in Baliunas et al. (1995). As can be seen from the table, the values derived here agree perfectly with those derived

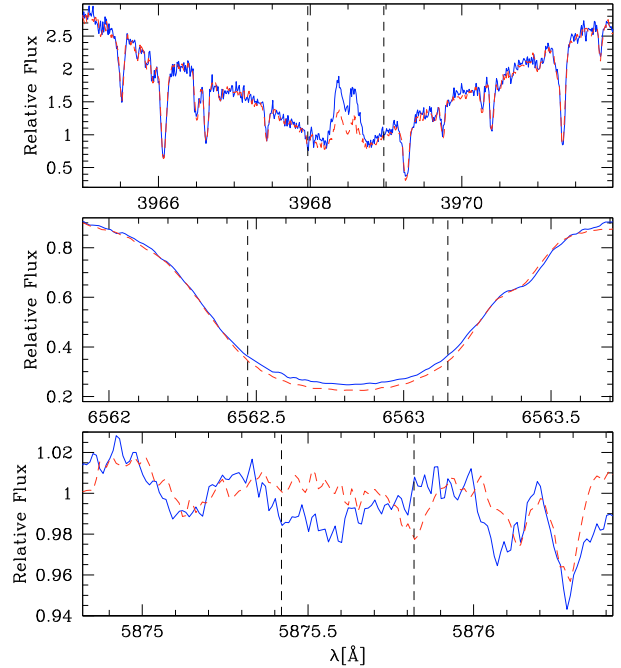


Fig. 1. Comparison of two spectra of HD 4628 near its maximum (blue continuous line) and minimum (red dashed line) activity level in the regions of the Ca II H line (top), the H_{α} line (middle), and the He I D3 line (lower panel). The vertical dashed lines denote the regions used to derive the activity indexes.

by Baliunas et al. This also reflects that, during the 5 years of measurements, we could follow a significant part of the stellar magnetic cycle. Except for HD 152391, all the stars seem to be in the low-activity side of the Vaughan-Preston gap (Vaughan & Preston 1980), and are thus similar to the Sun regarding their activity level.

The H_{α} index was derived by dividing the flux in the central 0.678 Å of the H_{α} line (6562.808 Å) by the flux in two reference windows between 6545.495–6556.245 and 6575.934–6584.684 Å. Finally, the He I D3 index was derived by dividing the flux in the 0.4 Å central region of the 5875.62 Å line by the flux in two 5 Å wide reference windows in each side of the line, centered on 5869 and 5881 Å.

While the Ca II H and K lines and H_{α} line typically present a re-emission at the center associated with activity phenomena, the depth of the He I D3 line increases in solar plages (Landman 1981). A correlation is thus expected to be present between the Ca II H and K index and the H_{α} index, while these two indexes will in principle be anti-correlated with the He I D3 activity indicator. This can be seen in Fig. 1, though from this plot is also

³ The calibration yields $S_{\text{MW}} = 30.985 \times S_{\text{HARPS}} + 0.042$.

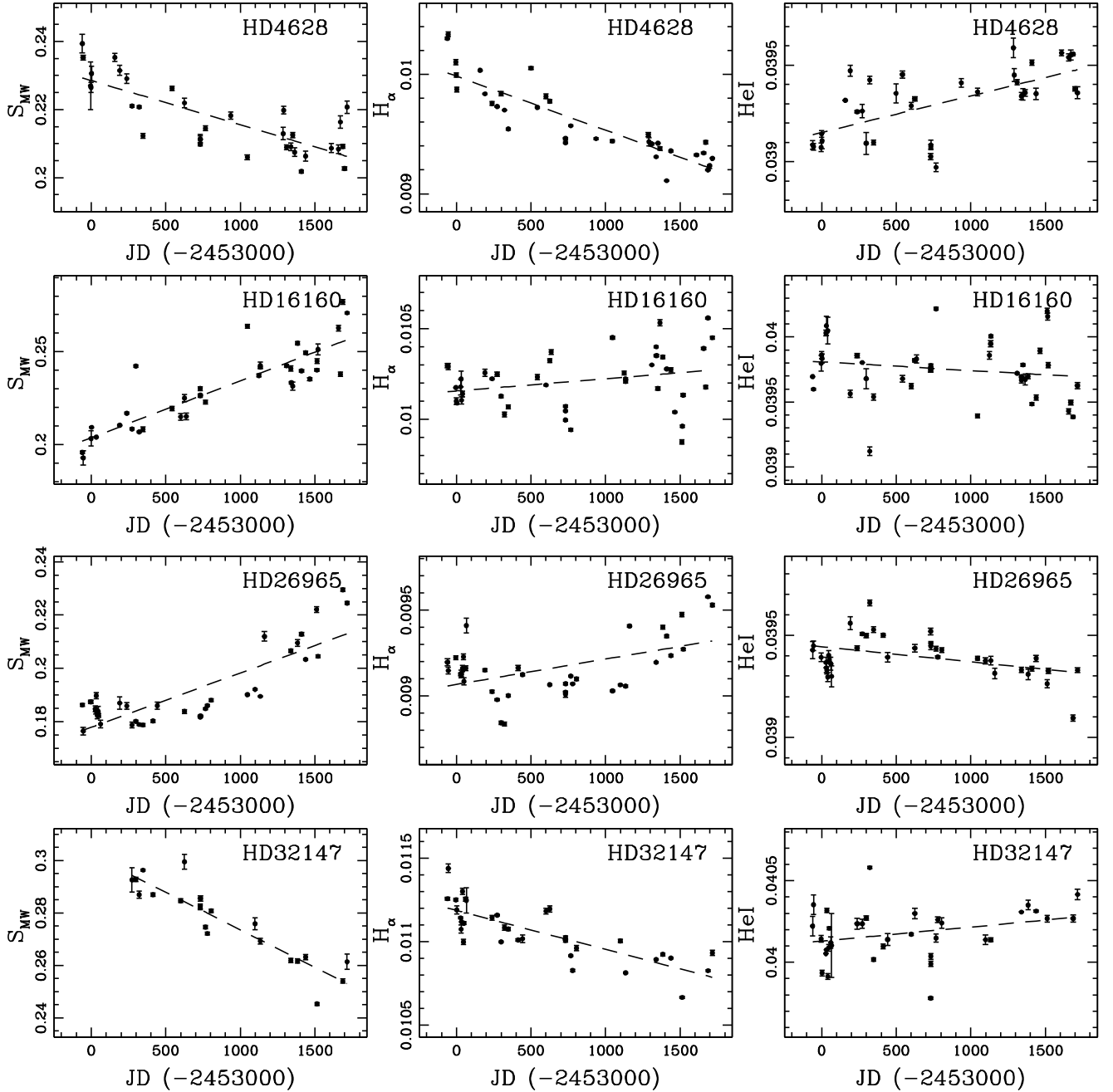


Fig. 2. Activity indexes for HD 4628, HD 16160 HD26965A, and HD 32146 as a function of time. *Left panels* denote variations in the Mount Wilson H and K “S” index, *middle panels* the H_{α} index, and the *right panels* the He I index. The dashed line represents a linear fit to the data. For comparison reasons, the x -scale was set constant in all the plots.

clear that the two former lines are more sensitive to activity variations than the latter one. This is partially caused by the weakness of the He I D3 line, which it is diluted by several atomic lines in the same region, and affected by telluric absorption features (Danks & Lambert 1985; Saar et al. 1997).

The wavelength region where the Ca II H and K lines are present (blue) often has a low S/N , making it difficult in some cases to derive a reliable activity index. Beyond this, and because the spectra were collected with a simultaneous ThAr wavelength calibration spectrum, contamination from the nearby ThAr order may in some cases alter the results. To avoid this, only spectra with an $S/N > 20$ near 4000 \AA were used to derive the Ca II H and K “ S_{HARPS} ” index.

5. Results

5.1. Activity cycle variations

In Figs. 2 and 3 we present time series of the three activity indexes for the 8 stars in our program⁴. Each point in the figure denotes the average of the measurements over one observing night (if multiple spectra existed for a given night). The error bars were computed using the dispersion of the different measurements in case several spectra per night were taken, or the individual error for nights when one single spectrum was obtained.

⁴ Data available in online Tables 5–7.

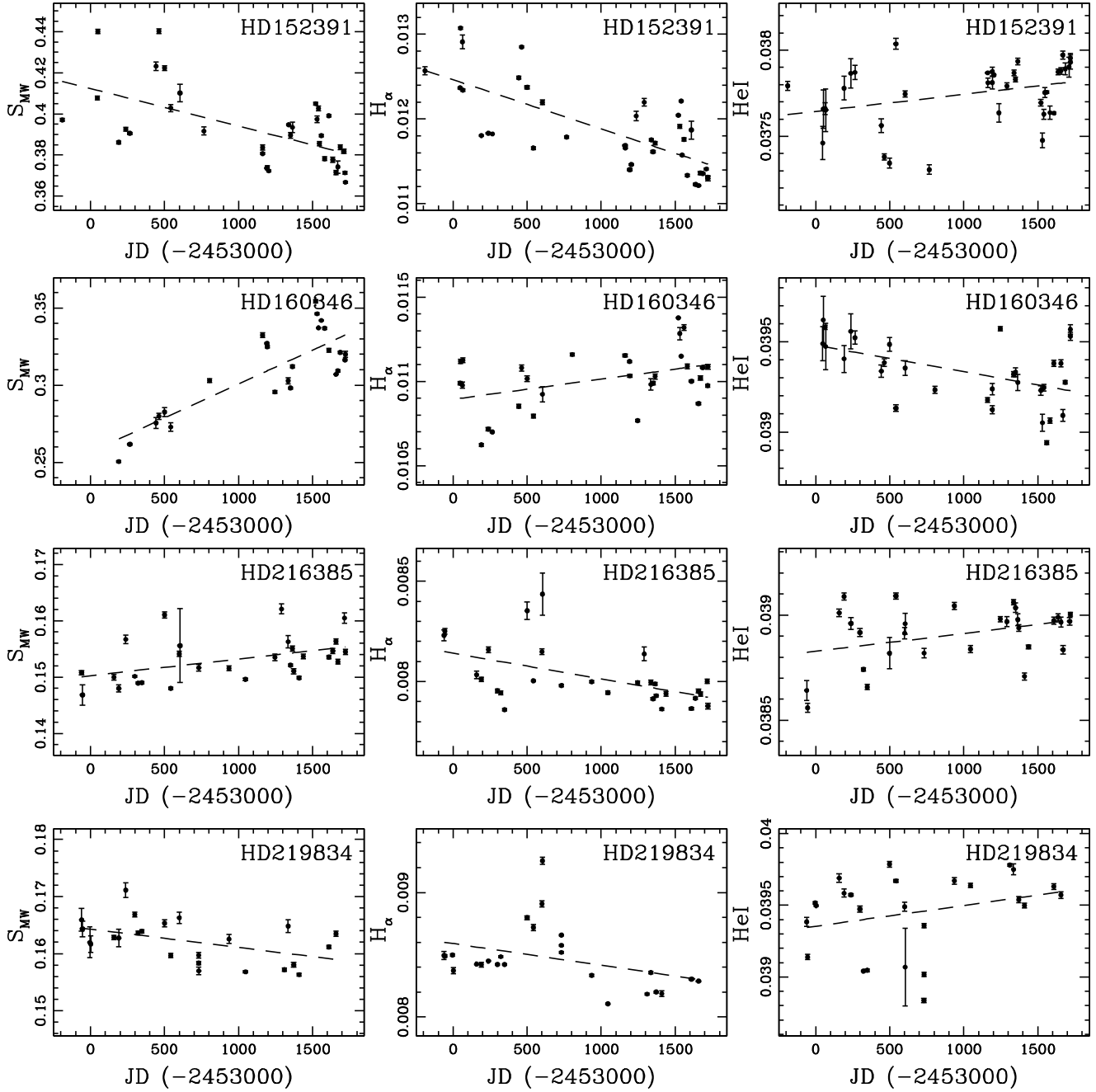


Fig. 3. Same as Fig. 2 for HD 152391, HD 160346, HD 216385, and HD 219834A.

A general look at the plots show that several of the stars present clear long-term activity cycle variations, as expected. In general also, these variations are seen in all the activity indexes (see also discussions in Livingston et al. 2007; Cincunegui et al. 2007; Meunier & Delfosse 2009), though the Ca II S index variations seem clearer and present smaller dispersion. Our data suggest, however, that all these indexes can be used to trace long-term activity variations in solar-type stars.

As mentioned above, the He I index is generally anti-correlated with the H_{α} and Ca II H and K indexes (the last two are generally correlated). This is expected from studies of the solar active regions (Landman 1981). The exception for this is the late F dwarf HD 216385. Though not the scope of the present paper, our results thus suggest that in F dwarfs the physics of the

formation of the He I line is different from the one seen for early-K dwarfs. This star presents, however, a very stable activity level throughout all the series of measurements, confirming its stability as shown in Baliunas et al. (1995) – it was actually included in our sample as a “standard”.

Some of the stars show higher frequency structure. This is likely due to the appearance and disappearance of activity phenomena such as spots and plages, and their modulation with stellar rotation. In the present paper we are mostly interested in long-term variations. We will leave the discussion of these high frequency variations to a different paper.

HD 219834A presents a clear spike in the H_{α} and He I indexes near JD \sim 2 453 600. As shown in Sect. 5.2, this star is a long-period binary with an eccentricity significantly different

Table 4. Orbital elements of the fitted orbits for HD 16160, HD 160346, and HD 219834. See text for more details.

Parameter	HD 16160	HD 160346	HD 219834 A	Units
P	21 900 [†]	83.7288 ± 0.0007	2338 ± 17	[d]
T	2 457 280 ± 271	2 454 590.40 ± 0.02	2 453 768 ± 19	[d]
a	14.0	0.36	4.10	[AU]
e	0.75 [†]	0.2048 ± 0.0004	0.184 ± 0.005	
V_r (HARPS)	25.53 ± 0.05	21.941 ± 0.002	10.56 ± 0.03	[km s ⁻¹]
ω	144 ± 2	140.1 ± 0.1	213.9 ± 0.7	[degr]
K_1	1052 ± 194	5691 ± 3	6017 ± 11	[m s ⁻¹]
$\sigma(\text{O-C})$	1.51	7.11	25.8	[m s ⁻¹]
N	78	33	25	
$m_2 \sin i$	74	101	448	[M_{Jup}]

Notes. ^(†) Fixed according to Golimowski et al. (2000).

from zero. A fit to the radial velocities shows that the periastron passage occurs near the above date. We may thus be seeing activity induced by the fainter secondary star on HD 219834A. This issue is beyond the scope of the present paper, but will be discussed in a separate work.

5.2. Multiple stars

Three of the stars in our sample are members of multiple stellar systems. To be able to study the influence that magnetic cycle variations may have on the measurement of RVs, we need to subtract the variations caused by the orbital period. In this section we describe the procedures used in each case.

5.2.1. HD 16160

HD 16160 (Gl 105 A) is member of a known triple system, with Gl 105 C orbiting Gl 105 A with a period of ~ 60 years, orbital eccentricity of ~ 0.75 , and with semimajor axis of ~ 15 AU (Golimowski et al. 2000). Since our data only cover a small part of the orbital phase, we used the radial-velocity measurements of this star presented by Golimowski et al.⁵, together with our own measurements, to fit a Keplerian function to the system and obtain a global orbital solution (see Table 4 and Fig. 4). In this process we fixed the orbital period and eccentricity to the values mentioned above. We used the residual radial velocities of this fit for the rest of the paper.

Leaving all the parameters free we find a slightly better solution with an orbital period $\sim 11\,000$ days, but this solution is not significantly better than the one adopted. Since our data, together with the one of Golimowski et al. (2000), do not cover one entire orbital period, we have no way to constrain the orbital solution using only radial velocities.

5.2.2. HD 160346

Halbwachs et al. (2003) used CORAVEL radial-velocity measurements with Hipparcos (ESA 1997) astrometry to conclude that HD 160346 (GJ 688) is a spectroscopic binary (SB1) with a period of 83.7 days, eccentricity of 0.20, and mass ratio M_2/M_1 of 0.5. A Keplerian fit to the HARPS radial velocities perfectly confirm this result (Table 4 and Fig. 5). The residuals around this Keplerian fit will be used for the rest of this work.

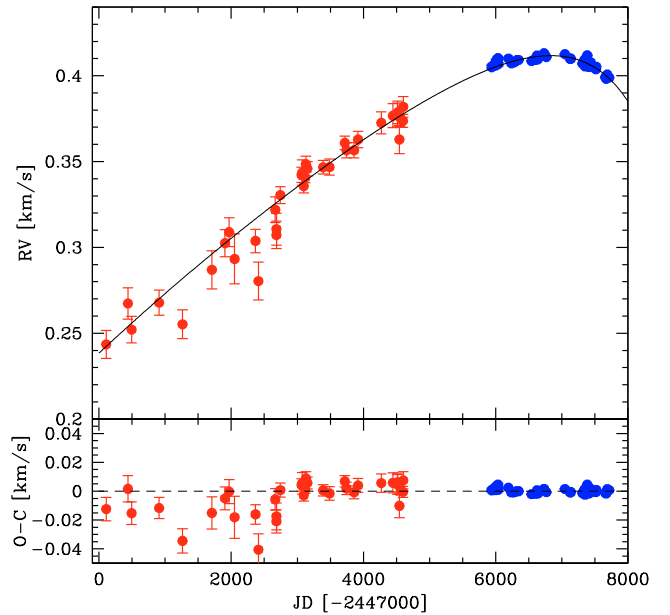


Fig. 4. Radial velocities of HD 16160 and best-fit Keplerian orbit. The lower panel presents the residuals of the fit.

5.2.3. HD 219834A

HD 219834A is a known hierarchical triple system, where the A component has been identified as a spectroscopic binary SB1 (Duquennoy & Mayor 1991; Tokovinin 1997). Our HARPS data perfectly confirm (and refine) the previously determined orbital parameters of the system. Our radial-velocities are best fit with a Keplerian function with a period of 2337 days, eccentricity 0.18, and semi-amplitude $K = 6.018$ km s⁻¹ (Table 4 and Fig. 6). This signal is compatible with a low mass ($0.43 M_{\odot}$ – minimum mass) stellar companion orbiting the slightly evolved $1.25 M_{\odot}$ star HD 219834A.

Unfortunately, the high residual velocities around the orbital fit (rms of ~ 25 m s⁻¹), together with their structure, strongly suggest that we are observing a blended spectrum and that HD 219834A is an SB2. Alternatively, additional companions could be present in the system. Better fits are indeed obtained with 2 or 3 Keplerian functions, but because our data barely covers one orbital period it does not allow us to find any convincing result.

⁵ Taken directly from their postscript figure.

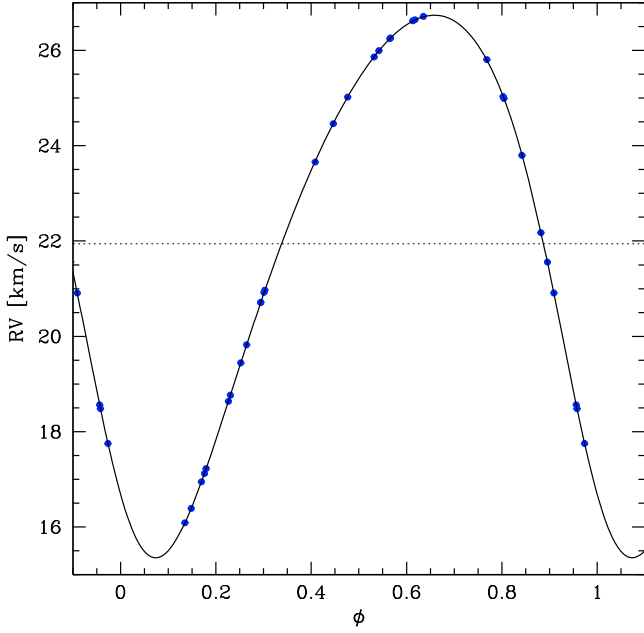


Fig. 5. Phase folded radial-velocities of HD 160346 and best-fit Keplerian orbit.

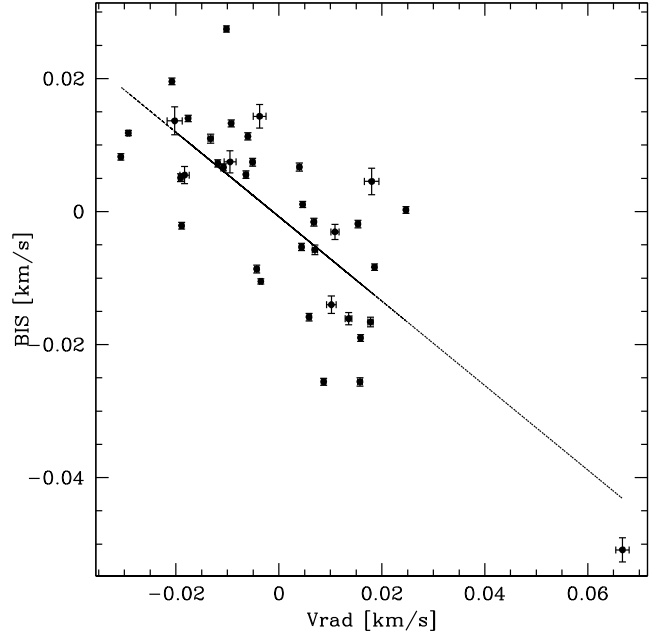


Fig. 7. Radial velocities vs. BIS for HD 152391.

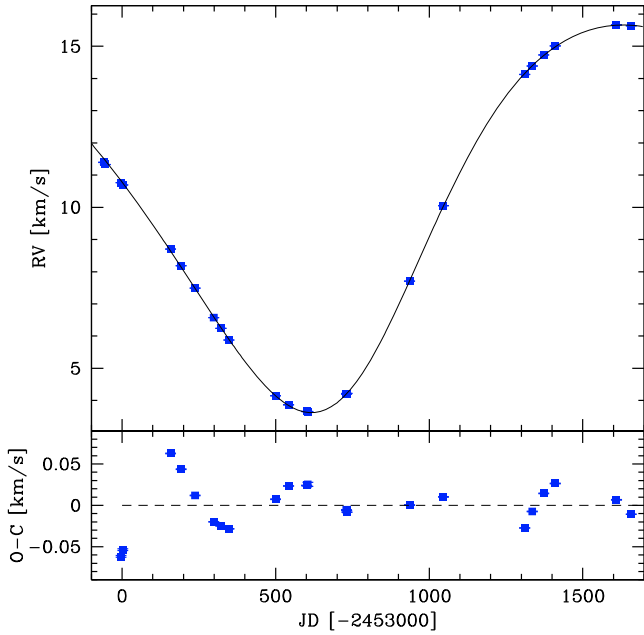


Fig. 6. Radial velocities of HD 219834A and best-fit Keplerian orbit. The lower panel presents the residuals of the fit.

These facts make it impossible to use the measurements of this star to study long-term and low-amplitude RV variations. We have thus excluded the data of HD 219834A for the rest of the paper.

5.3. HD 152391

HD 152391 is the most active star in our sample. As expected, a look at the obtained RVs reveal a high noise level close to 18 m s^{-1} . A clear correlation between the velocities and BIS is also seen (Fig. 7). As for other similar stars (such as HD 166435 – [Queloz et al. 2000](#)), this seems to indicate that the

observed radial-velocity variations are being induced by photospheric features like spots. In contrast to the case of HD 166435, however, we could not find any clear periodicity in the data.

We tried to correct the radial-velocities using the relation between BIS and RV, a procedure already successfully used by [Melo et al. \(2007\)](#). However, the rms around the average velocity only decreased slightly to $\sim 12.5 \text{ m s}^{-1}$. This high value makes the search for any low-amplitude and long-term signal very difficult. We thus decided to keep this star out of the rest of the discussion.

5.4. Activity, radial-velocity, and CCF parameters

After removing HD 152391 and HD 219834A from the list (see discussion above), we are left with 6 objects (HD 4628, HD 16160, HD 26965A, HD 32147, HD 160346, and HD 216385) for which we can study the influence of activity cycle variations on the measured radial velocities.

We searched the literature for references to multiplicity among these targets. Except for HD 16160 and HD 160346 (see discussion above), none of the remaining stars has any reference for a short-period (up to a few years) companion. HD 26965A is member of a known triple system, with a long period of ~ 8000 years ([Heintz 1974](#)). HD 216385 is also known to be member of a common proper motion pair with the second star situated 250 arcsec away ([Lépine & Bongiorno 2007](#)); at a distance of ~ 26 pc, this corresponds to a projected separation of ~ 6500 AU. For HD 4628, HD 26965A, HD 32147, and HD 216385 we thus have no indication that radial-velocity variations induced by a stellar companion can be detectable in our 5-year baseline.

5.4.1. Activity and CCF parameters

In Fig. 8 we present the yearly average time series of the S_{MW} , radial-velocity, BIS, and the CCF's contrast and FWHM⁶. In the plot, the dashed lines represent linear fits to the data. Each point

⁶ Data available in online Table 8.

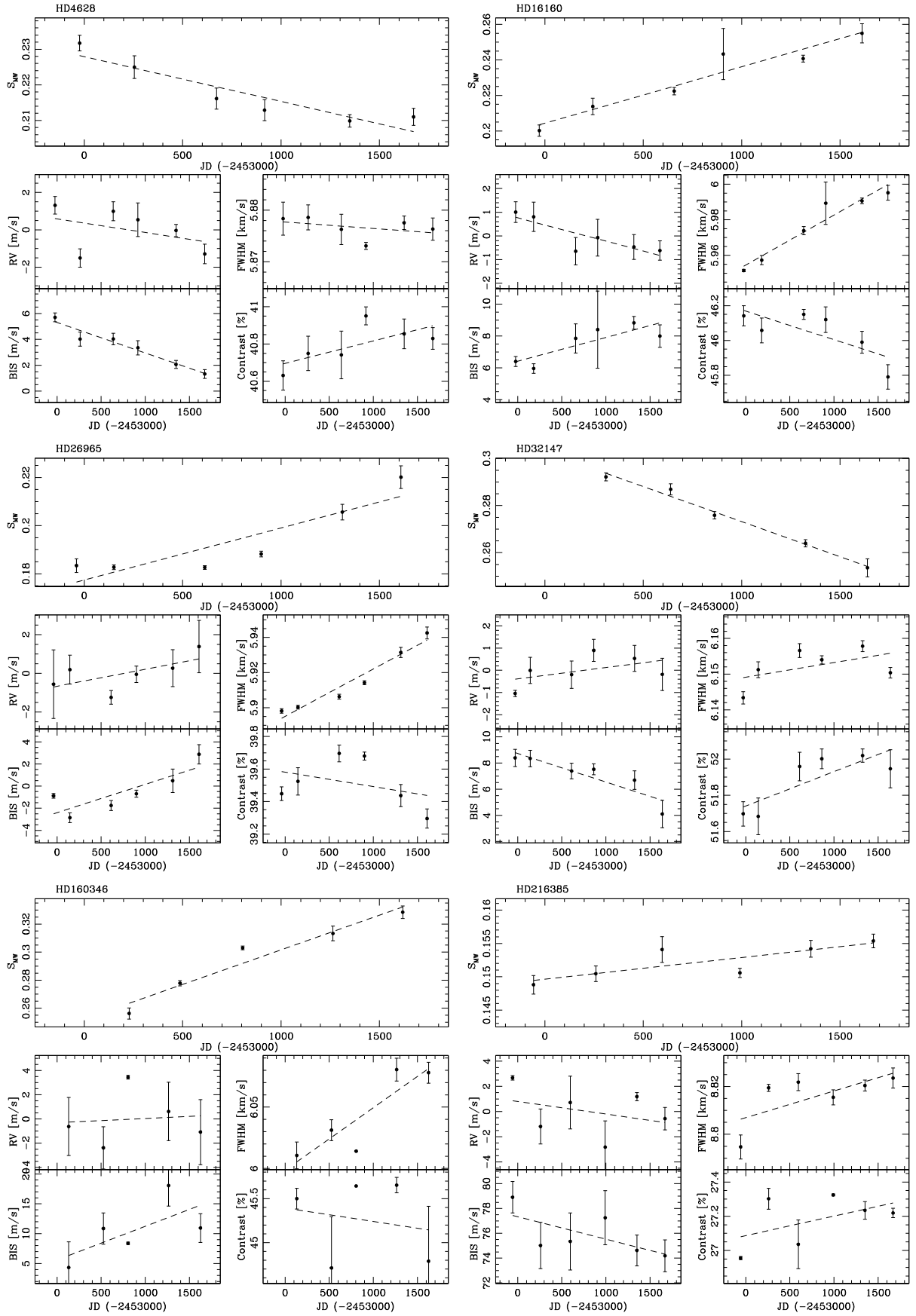


Fig. 8. Yearly average S_{MW} (in each top panel), radial-velocity, BIS, and the Cross-Correlation Function's Contrast and FWHM function of time for HD 4628, HD 16160 and HD 26965A, HD 321467, HD 160346, and HD 216385. For comparison reasons the x-scale was set constant in all the plots.

in the plot corresponds to the average of the values in time bins corresponding to the years 2003 to 2008. The error bars are computed as the rms/\sqrt{N} , where N is the number of measurements in each window. The average Julian Date for each bin was considered for plotting reasons. The third date for HD 160346 (corresponding to the year 2006) has no error bar for FWHM and contrast, since only one measurement of this star was available in that year (no error bars are provided by the HARPS pipeline for these two parameters). For HD 32147, none of the available spectra obtained in 2003 was good enough for deriving a reliable “S” value, though radial-velocity measurements exist.

The first remarkable result that comes out of the plots is that in most cases there seems to be a clear positive correlation between the S_{MW} index and both the FWHM (the only exceptions are HD 32147 and our “standard” HD 216385) and the BIS of the HARPS CCF. In other words, the FWHM and the BIS seem to be good indicators of the stellar activity level. The opposite trend (anti-correlation) is seen between S_{MW} and the CCF’s contrast. For HD 26965 A these relations are particularly clear since the curvature observed in the S_{MW} variation is also clearly observed in the different CCF parameters.

The reason for these facts is not fully clear, but they suggest that these CCF parameters can be used as a proxy for the chromospheric activity level of a solar-type star. In particular, they can be used to follow the activity cycle variations of the targets in complement to measurements of different activity indexes.

Boisse et al. (2009) have shown that the parameters of the CCF, in particular its contrast, vary as a function of the activity level of the star for the very active planet host HD 189733. The CCF appears to be shallower when the star is more active. These authors explain this variation by dark spots (typically associated with stellar activity) that have a spectrum that is different from the one emitted by the remaining stellar photosphere. These features will thus naturally induce changes in the overall spectrum that are noticeable in the shape of the CCF. We should note, however, that spots also influence the wings of spectral lines (decreasing their intensity), thus decreasing their FWHM. In this case an anti-correlation between FWHM and activity level could be expected.

The results presented here confirm the conclusions of Boisse et al. (2009). Interestingly, however, our results further suggest that these changes are detectable even in inactive (solar-like) stars, such as the 6 objects discussed in this section.

Variations in the CCF contrast and FWHM can also be induced when the cores of stronger lines start to fill as the star becomes more active. This will make the lines (and consequently the CCF) shallower, and since the FWHM is measured at a lower level (closer to continuum), its value will also increase.

We add that a change in the shape of the CCF can also be induced by variations in the convection pattern (Dravins 1982). Observations show that solar line bisectors smaller lower velocity spans and convective blueshifts in active regions (Livingston 1982; Brandt & Solanki 1990). This could explain the observed variations in the shape of the CCF as a function of the activity level of the star.

5.4.2. Activity and radial velocity

If on the one side activity cycle variations seem to induce clear signals on the above discussed CCF parameters (FWHM, Contrast, and BIS), the situation regarding the RV is not so clear. For HD 26965 A we find a positive correlation between the “ S_{MW} ” index (that varied by ~ 0.04) and the RV. Interestingly,

there is a slight indication that a change in slope of the RV time series exists accompanying the observed variation in “S”. The same positive correlation is observed for HD 4628, though in this case the RV seems to present a higher dispersion. This may also be caused by HD 4628 presenting a lower amplitude variation in its activity level ($\Delta S \sim 0.02$, between the first and last years of measurements).

The opposite trend, however, is found for HD 16160, where the “S” index increased monotonically by about 0.054 during the period of our measurements. For this case we cannot fully exclude that a slightly wrong orbital fit could have left any trend in the residuals.

For HD 32147 ($\Delta S \sim 0.04$) and HD 160346 ($\Delta S \sim 0.07$), both showing clear and monotonic variation in the “S” index, no significant RV variation is observed in our data. Finally, for HD 216385, only a small “ S_{MW} ” variation is observed (0.006). We note that this star shows very small long term chromospheric activity variation. It was actually included in our sample for its constancy in S_{MW} (Baliunas et al. 1995). This is also the only F-type star in our sample.

As a test, we computed the Spearman rank correlation coefficient for the “ S_{MW} ” vs. RV relation. A Monte-Carlo test, where we generated random RV and “ S_{MW} ” values with the same rms as the original sample shows that, in most cases, a higher correlation can be found in more than 10% of the random samplings. The only exception is HD 26965 A, for which a false alarm probability of 1.5% exists. The fact that we only have a few data points precludes any firm conclusions on this.

In face of the present (and contradictory) results, we cannot conclude anything about the existence of radial-velocity variations induced by long-term changes in the chromospheric activity level in our sample of early-K dwarfs. More data is clearly needed, and in particular we need to cover the whole magnetic cycles of the target stars better. The study of a larger sample could also be important. In any case, our results suggest that long-term variations significantly above $\sim 1 \text{ m s}^{-1}$ can be excluded in our targets as being caused by variations in the chromospheric activity level during the stellar magnetic cycle.

We also cannot exclude the possibility that some of the observed RV variations are being caused by the presence of long-period companions, either planets or stellar in nature. A deep adaptive optics search for close companions to our targets may be crucial for clarifying this aspect.

6. Discussion and conclusions

In this paper we present the results of a long-term project to investigate the effect that long-term stellar magnetic cycles may have on the measurement of precise radial velocities. For this we observed a sample of 7 late-G or early-K dwarfs and one late F dwarf (an activity “standard”) for more than 5 years with the HARPS spectrograph. The obtained spectra allowed us to derive a precise value from each spectrum for the RV, a measurement of the chromospheric activity level using 3 different spectral indexes (CaII “S”, H_{α} , and He I), as well as several parameters of the CCF (BIS, FWHM, and contrast). The results of this survey suggest that in our sample:

- All the three activity indexes measured are good tracers of stellar activity level variations along the magnetic cycle, though the CaII “S” index presents the smallest dispersion. In general, the CaII “S” and H_{α} indexes are correlated with each other, while the He I is anti-correlated with the first two.

- The activity level variations are also clearly reflected in the values of BIS, FWHM, and contrast of the HARPS CCF. The values of BIS are particularly sensitive to activity level variations. This suggests that measurements of these parameters can be used to clearly diagnose long-term variations in the chromospheric level of a star. The measurement of BIS, FWHM, and contrast may even likely be useful to correct the velocity measurements for the effect of long-term stellar activity (Saar & Fischer 2000), in a similar way to one used by Melo et al. (2007) to correct for higher frequency noise. These results may be of extreme importance for present and future high-precision RV planet searches.
- Although some of our targets show hints of low-amplitude (at the $\sim 1 \text{ m s}^{-1}$ level) and long-term RV variations that could be caused by variations in the activity level of the star, our results are not conclusive about the nature and amplitude of this effect. Our data suggests that for early-K dwarfs the variation in the stellar activity level along the magnetic cycles does not strongly induce variations in the measured RVs. Early-K dwarfs are thus bona fide targets to search for very low-mass planets using precise radial velocity instruments. We note that these targets already have the lowest granulation and oscillation “noise” level among solar type stars (Dumusque et al., in preparation).

A better understanding of the influence of long-term stellar magnetic cycles on the radial-velocities is certainly crucial to plan future radial-velocity planet searches with a new generation of instruments like ESPRESSO@VLT⁷ or CODEX@E-ELT (Pasquini et al. 2008). These instruments will be able to obtain RVs with a precision of better than 10 cm s^{-1} , allowing the detection of Earth-like planets in the habitable zone of nearly solar-type stars.

To further investigate the above discussed issues, a continuation of the present program is needed. Furthermore, it would be very important to extend our sample to earlier type G-dwarfs (more similar to our Sun). Convective blueshifts are lower in K-dwarfs than in F- and G-dwarfs (Gray 1992). In active regions the convective velocities are lower, also implying smaller line asymmetries (Livingston 1982; Brandt & Solanki 1990). We may thus expect a stronger effect of chromospheric activity for earlier type dwarfs (e.g. Saar 2009).

As a complement, it would also be important to investigate the existence of long period stellar companions in detail, which could be able to induce long-term RV variations. An adaptive optics survey should thus be conducted to investigate this possibility.

Acknowledgements. We would like to thank our referee, S. Saar, for the very positive and helpful report. N.C.S. would like to acknowledge the support by the European Research Council/European Community under the FP7 through a starting grant, as well from Fundação para a Ciência e a Tecnologia (FCT), Portugal, through program Ciência 2007, and in the form of grants PTDC/CTE-AST/098528/2008 and PTDC/CTE-AST/098604/2008. J.G.S. would like to acknowledge the support by EC’s FP6 and by FCT (with POCI2010 and FEDER funds), within the HELAS international collaboration.

References

- Baliunas, S. L., Donahue, R. A., Soon, W. H., et al. 1995, *ApJ*, 438, 269
 Baliunas, S., Sokoloff, D., & Soon, W. 1996, *ApJ*, 457, L99
 Boisse, I., Moutou, C., Vidal-Madjar, A., et al. 2009, *A&A*, 495, 959
 Bonfils, X., Mayor, M., Delfosse, X., et al. 2007, *A&A*, 474, 293
 Bouchy, F., Pont, F., Santos, N. C., et al. 2004, *A&A*, 421, L13
 Brandt, P. N., & Solanki, S. K. 1990, *A&A*, 231, 221
 Cincunegui, C., Díaz, R. F., & Mauas, P. J. D. 2007, *A&A*, 469, 309
 Danks, A. C., & Lambert, D. L. 1985, *A&A*, 148, 293
 Dravins, D. 1982, *ARA&A*, 20, 61
 Duquenois, A., & Mayor, M. 1991, *A&A*, 248, 485
 ESA 1997, The Hipparcos and Tycho Catalogues
 Fernandes, J., & Santos, N. C. 2004, *A&A*, 427, 607
 Flower, P. J. 1996, *ApJ*, 469, 355
 Golimowski, D. A., Henry, T. J., Krist, J. E., et al. 2000, *AJ*, 120, 2082
 Gray, D. F. 1992, *The Observation and Analysis of Stellar Photospheres*, ed. D. F. Gray (Cambridge, UK: Cambridge University Press), June, 470
 Halbwachs, J. L., Mayor, M., Udry, S., & Arenou, F. 2003, *A&A*, 397, 159
 Heintz, W. D. 1974, *AJ*, 79, 819
 Huélamo, N., Figueira, P., Bonfils, X., et al. 2008, *A&A*, 489, L9
 Kürster, M., Endl, M., Rouesnel, F., et al. 2003, *A&A*, 403, 1077
 Kurucz, R. 1993, *ATLAS9 Stellar Atmosphere Programs and 2 km s⁻¹ grid*, Kurucz CD-ROM, Cambridge, Mass., Smithsonian Astrophysical Observatory, 13
 Landman, D. A. 1981, *ApJ*, 244, 345
 Lépine, S., & Bongiorno, B. 2007, *AJ*, 133, 889
 Livingston, W. C. 1982, *Nature*, 297, 208
 Livingston, W., Wallace, L., White, O. R., & Giampapa, M. S. 2007, *ApJ*, 657, 1137
 Mayor, M., & Queloz, D. 1995, *Nature*, 378, 355
 Mayor, M., Bonfils, X., Forveille, T., et al. 2009, *A&A*, 507, 487
 McMillan, R. S., Moore, T. L., Perry, M. L., & Smith, P. H. 1993, *ApJ*, 403, 801
 Melo, C., Santos, N. C., Gieren, W., et al. 2007, *A&A*, 467, 721
 Meunier, N., & Delfosse, X. 2009, *A&A*, 501, 1103
 Noyes, R. W., Hartmann, L. W., Baliunas, S. L., Duncan, D. K., & Vaughan, A. H. 1984, *ApJ*, 279, 763
 Pasquini, L., Avila, G., Delabre, B., et al. 2008, in *Precision Spectroscopy in Astrophysics*, ed. N. C. Santos, L. Pasquini, A. C. M. Correia, & M. Romaniello, 249
 Paulson, D. B., Saar, S. H., Cochran, W. D., & Hatzes, A. P. 2002, *AJ*, 124, 572
 Pepe, F., Mayor, M., Rupprecht, G., et al. 2002, *The Messenger*, 110, 9
 Queloz, D., Mayor, M., Weber, L., et al. 2000, *A&A*, 354, 99
 Queloz, D., Henry, G. W., Sivan, J. P., et al. 2001, *A&A*, 379, 279
 Saar, S. H. 2009, in *Am. Inst. Phys. Conf. Ser.*, ed. E. Stempels, 1094, 152
 Saar, S. H., & Donahue, R. A. 1997, *ApJ*, 485, 319
 Saar, S. H., & Fischer, D. 2000, *ApJ*, 534, L105
 Saar, S. H., Huovelin, J., Osten, R. A., & Shcherbakov, A. G. 1997, *A&A*, 326, 741
 Santos, N. C., Mayor, M., Naef, D., et al. 2000, *A&A*, 361, 265
 Santos, N. C., Bouchy, F., Mayor, M., et al. 2004a, *A&A*, 426, L19
 Santos, N. C., Israelian, G., & Mayor, M. 2004b, *A&A*, 415, 1153
 Schaller, G., Schaefer, D., Meynet, G., & Maeder, A. 1992, *A&AS*, 96, 269
 Schaefer, D., Charbonnel, C., Meynet, G., Maeder, A., & Schaller, G. 1993a, *A&AS*, 102, 339
 Schaefer, D., Meynet, G., Maeder, A., & Schaller, G. 1993b, *A&AS*, 98, 523
 Snenen, C. 1973, Ph.D. Thesis, Univ. of Texas
 Sousa, S. G., Santos, N. C., Mayor, M., et al. 2008, *A&A*, 487, 373
 Tokovinin, A. A. 1997, *A&AS*, 124, 75
 Udry, S., & Santos, N. 2007, *ARA&A*, 45, 397
 Vaughan, A. H., & Preston, G. W. 1980, *PASP*, 92, 385
 Vaughan, A. H., Preston, G. W., & Wilson, O. C. 1978, *PASP*, 90, 267
 Wright, J. T., Marcy, G. W., Butler, R. P., et al. 2008, *ApJ*, 683, L63

⁷ <http://espresso.astro.up.pt>